Science Press

Available online at www.sciencedirect.com

SCIENCE DIRECT®

Trans. Nonferrous Met. Soc. China 18(2008) 1−5

Transactions of Nonferrous Metals Society of China

www.csu.edu.cn/ysxb/

Dynamic property evaluation of aluminum alloy 2519A by split Hopkinson pressure bar

ZHANG Xin-ming(张新明), LI Hui-jie(李惠杰), LI Hui-zhong(李慧中), GAO Hui(高　慧), GAO Zhi-guo(高志国), LIU Ying(刘　瑛), LIU Bo(刘　波)

School of Materials Science and Engineering, Central South University, Changsha 410083, China

Received 13 March 2007; accepted 28 June 2007

Abstract: Impact behavior of aluminum alloy 2519A was investigated at strain rates of 600−7 000 s^{-1} and temperatures of 20−450 ℃ by a split Hopkinson pressure bar. The results show that the flow stress is dominated by temperature, and it increases with strain rate and decreases with deformation temperature. The serrated flow curves show the dynamic recrystallization occurs. The strain rate sensitivity exponents *m* determined are 0.066, 0.059 4, 0.059 0 and 0.057 3 at 20, 150, 300 and 450 ℃, respectively. Cowper- Symonds constitutive equation expressing the plastic flow behavior was calculated by analysis and regression of the experimental results. The fracture characteristics under the experimental conditions were observed by optical microscopy(OM) and scanning electron microscopy(SEM). It is determined that the tested material fails as a result of adiabatic shearing.

Key words: aluminum alloy 2519A; split Hopkinson pressure bar; dynamic recrystallization; strain rate; adiabatic shearing

1 Introduction

Aluminum alloy 2519, which has been developed into aluminum alloy 2519A, has been used extensively in naval structures, such as advanced amphibious assault vehicle(AAAV) because of its high specific strength and good corrosion resistance. An amount of work has been carried out on the plastic flow of 2519A alloy at low strain rates and various temperatures. LI et al[1] determined the stress—strain curves and thermally-activated parameter at temperatures ranging from 300 to 450 ℃ and strain rates from 0.01 to 10 s^{-1}. LIN et al[2] have studied the stress—strain curves at temperatures ranging from 300 to 450 ℃ and strain rates from 0.05 to 25 s^{-1}. However, there is little information about systematic effects of strain rate and temperature on the plastic flow response of this alloy during dynamic impact plastic deformation.

The split Hopkinson pressure bar(SHPB) has been widely used to determine mechanical properties of materials at high loading rates[3], with which impact deformation responses of many kinds of aluminum alloys, such as AA2024[4], AA5754 and AA5182[5], AA5083 [6], AA6005-T6[7] and 7075[8], have been studied at high strain rate. Positive strain rate sensitivity at high strain rates has been interpreted by different deformation mechanisms, such as thermal activating mechanism, the enhanced rate of dislocation generation[9] and viscous drag mechanism[10]. Under high strain rate loading, the plastic deformation can be regarded an adiabatic process, accompanied by a significant temperature rise. Severe plastic deformation is restricted to a narrow region that is generally referred to as adiabatic shear band(ASB)[9,11]. Furthermore, internal cracks will often occur within ASBs and become the sites of eventual failure of material.

This work is to investigate the dynamic behavior of aluminum alloy 2519A by SHPB at temperatures ranging from 20 to 450 ℃, and strain rates ranging from 600 to 7 000 s^{-1}. The stress—strain relation and the fracture characteristics are described. A constitutive equation expressing the plastic flow behavior is suggested by analysis and regression of the test results.

Foundation item: Project(2005CB623706) supported by the National Basic Research Program of China
Corresponding author: ZHANG Xin-ming; Tel: +86-731-8830265; E-mail: xmzhang@mail.csu.edu.cn

2 Experimental

Cylindrical compression specimens of *d* 8 mm×6 mm and *d* 6 mm×4 mm were prepared from a 20 mm-thick 2519A-T87 plate with compositions given in Table 1.

Table 1 Chemical compositions of studied alloy (mass fraction, %)

Cu	Mg	Mn	V	Ti
5.8	0.2	0.30	0.06	0.05

Zr	Fe	Si	Al
0.20	0.20	0.10	Bal.

Dynamic compression at the high strain rates ranging from 600 to 7 000 s^{-1} and temperatures from 20 to 450 ℃ was performed by SHPB comprising an incident bar, a transmission bar made from 14.5 mm diameter maraging steel, and a striker bar. During compression, the specimens were located between the incident and the transmitted bar. The influence of friction was reduced by spreading a viscous lubrication cream. When the striker bar impacted the incident bar, rectangular stress pulse was generated and traveled along the incident bar until it hit the specimen. Part of the incident stress pulse was reflected from the bar/specimen interface, and a part of it was transmitted through the specimen. The transmitted pulse emitted from the specimen traveled along the transmitted bar. The incident, reflected and transmitted waveforms were measured using the strain gauges located on each bar. Two strain gauges were used in a half-bridge configuration to cancel out any possible bending. The stress, strain and strain rate of the specimen can be obtained by using the classical Hopkinson equations [12].

Dynamic testing at elevated temperatures was conducted in a radiant-heating furnace. The incident and reflected wave signals were recorded at the experimental temperatures and compared with those at ambient temperature. There was no apparent distortion due to any increase in temperature at the bar ends. The microstructure was examined for three specimens tested at each set of conditions using OM and SEM. Specimens were polished conventionally and etched with Kellor etchant composed of 95 mL H_2O, 2.5 mL HNO_3, 1.5 mL HCl, and 1.0 mL HF.

3. Results and discussion

3.1 Stress—strain behavior

True stress—strain curves of aluminum alloy 2519A at 150, 300 and 450 ℃ under strain rates of 630, 4 300 and 5 800 s^{-1} are shown in Fig.1. At each strain rate, the alloy exhibits an elastic stage in the initial stage of deformation and then yields, coming into a plastic stage. The flow curves demonstrate a wavy response, which can be associated with dynamic recrystallization (DRX). With the impact plastic deformation, dynamic recovery caused by cross-sliding of screw dislocations and climbing of edge dislocations is limited, and subgrain boundaries are not clearly formed. Therefore,

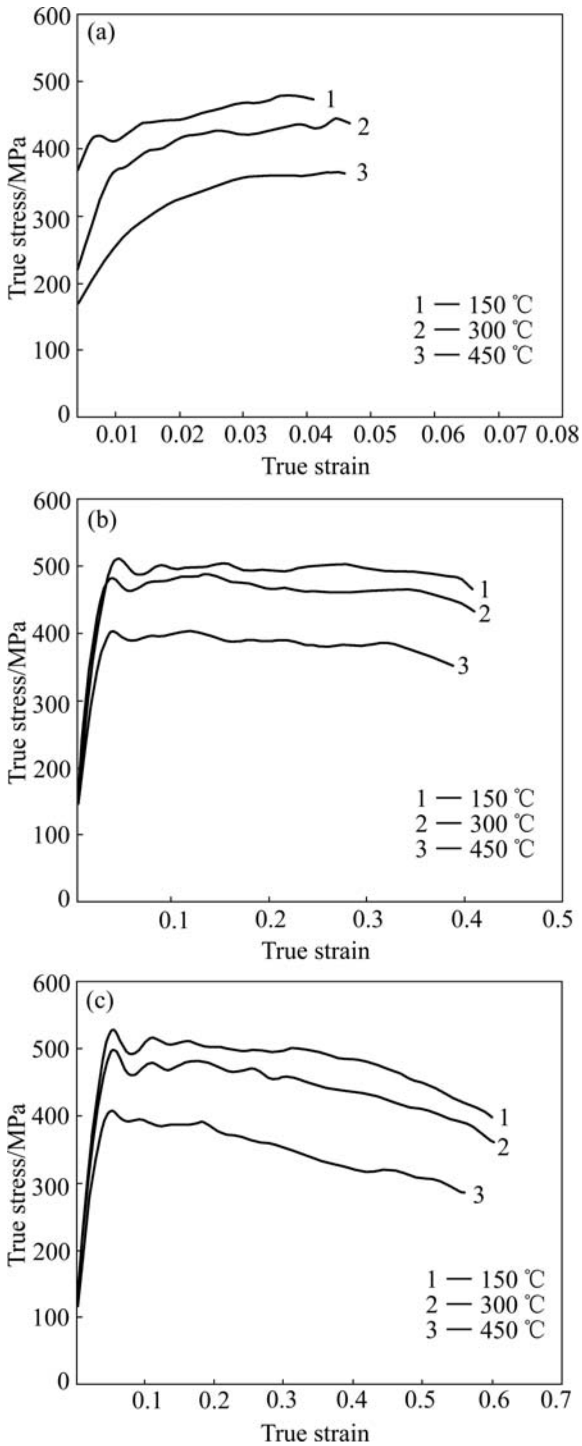

Fig.1 True stress—strain curves of specimens impacted at temperatures of 150, 300 and 450 ℃: (a) 630 s^{-1}; (b) 4 300 s^{-1}; (c) 5 800 s^{-1}

the density of dislocations still keeps high, which results in the rapid increment of stored energy. As soon as the stored energy in deformed metal reaches a critical value, dynamic recrystallization occurs. Furthermore, changes in strain rate have a significant effect on slope of flow curves: at the strain rate of 630 s^{-1}, the slope in the plastic region is positive but considerably small at temperatures considered. Work hardening caused by mutual intersection of the pinned dislocations resulted from increased dislocations density is beyond DRX-softening. When the impacts occur at strain rate of 4 300 s^{-1} and three temperatures, a nearly horizontal line is obtained, suggesting that the stress reaches a peak followed by a steady state deformation, in which increment, annihilation and rearrangement of dis-locations caused by interaction of them reach a dynamic balance. At strain rate of 5 800 s^{-1}, the stress reaches a peak followed by a decrease with increasing the strain at three temperatures. This result can be attributed to the adiabatic shearing thermal-plastic instability.

3.2 Influence of strain rate and temperature

As can be seen in Fig.1, the strain rate and temperature have marked influence on the flow stress. Fig.2 shows a plot of yield stress versus strain-rate for all the temperatures considered. It is clear that the relationship between the true stress and the strain rate at the given temperatures is represented by a single straight line, the slope of which gives the value *m* about the rate sensitivity of the flow stress. This type of stress—strain rate relationship has been reported for many aluminum alloys[4−8]. Fig.2 shows that aluminum alloy 2519A exhibits a mild increase in stress with strain rates at the temperatures considered. The strain rate sensitivity exponents *m* determined for the yield stress are 0.066, 0.059 4, 0.059 0 and 0.057 3, respectively, and the stress is proportional to the logarithm of the strain rate. This is generally due to the role of thermal activation in control of deformation mechanisms[13−14]. In addition, at 450 ℃, the flow stress is found to be relatively less sensitive to the strain rate, which suggests that thermal softening plays a major role in the strain-rate effect for higher temperature regions.

For all the specimens, the stress decreases markedly with increase of temperature; particularly, from 300 ℃ to 450 ℃, the stress decreases sharply. Since aluminum alloy 2519A is strengthened by the precipitates that form supersaturated solid solution during the decomposition of α(Al), the strength of material results from lattice strain interactions between the precipitates and the dislocations. During high-temperature loading, coarsening and dissolution of the precipitates coexist in the thermally-activated process. Increasing the deforma-tion temperature accelerates precipitates dissolution and

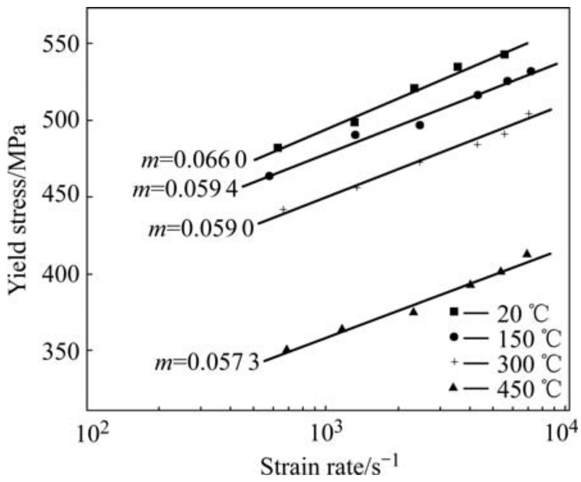

Fig.2 Influence of strain rate on yield stress as function of temperature

dislocation annihilation. These physical and metallurgical reactions result in the reduction of flow stress and strength. Although high rate deformation leads to an enhancement of strength due to the increase of work hardening and dislocation density, it is obvious that the deformation resistance of aluminum alloy 2519A is dominated by temperature effect.

3.3 Deformation constitutive equation

Computer simulations have been used extensively to predict the responses of complex structures at high strain rates. To ensure the reliability of the simulation results, it is necessary to determine the material's constitutive equation that contains specific material constants and parameters obtained experimentally. Many material constitutive models including “single-factor” and “multi-factor” have been proposed previously to describe the rate-dependent behaviors of metals[15]. The “multi-factor” material constitutive model includes strain, strain rate and temperature variables, however, it is quite difficult to establish. The “single-factor” material constitutive model includes one of these variables. The Cowper-Symonds overstress power law model, as shown in Eqn.(1), is often used for most structure materials [16]:

$$\frac{Y_\mathrm{d}}{Y}=1+\left(\frac{\dot{\varepsilon}}{B}\right)^{1/q} \tag{1}$$

where Y_d is the dynamic yield stress; Y is the static yield stress that is equal to 420 MPa for aluminum alloy 2519A; $\dot{\varepsilon}$ is the strain rate; B and q are material parameters.

Eqn.(1) can be used to predict the high strain rate deformation behavior of this alloy. Experimental data are used to determine the coefficients and exponents. The determined values of two specific material parameters for Al alloy 2519A are B=147 394.015 41 and q= 3.203 71. By putting the two material parameters into the Eqn.(1), the concrete Eqn.(2) is obtained, and Fig.3 shows the comparison of the measured curve tested at 20 ℃:

$$Y_{\mathrm{d}}=420\left[1+\left(\frac{\dot{\varepsilon}}{147\,394.015\,41}\right)^{1/3.203\,71}\right] \tag{2}$$

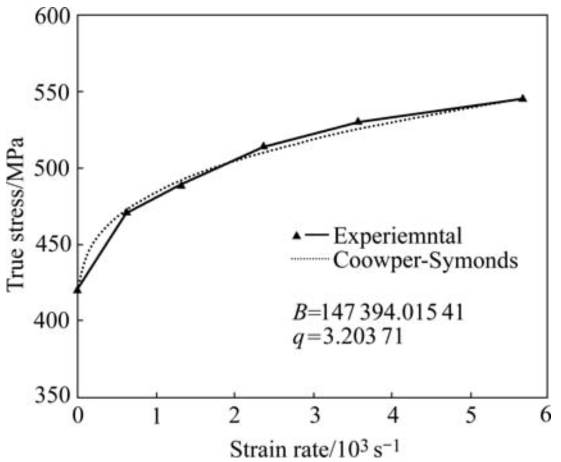

Fig.3 Comparison of simulated curve with measured curve at 20 ℃

3.4 Observations of fracture characteristics

In addition to plastic flow, damage and fracture are important to material dynamic characterization. Fractographic examination of the impacted material reveals that adiabatic shearing is the main fracture mechanism at strain rate of 5 800 and 7 000 s^{-1}. The specimen fails along planes inclined at approximate 45° to impact direction (i.e. along the plane of maximum shear stress). Fig.4 demonstrates the fracture features and orientation of ASB.

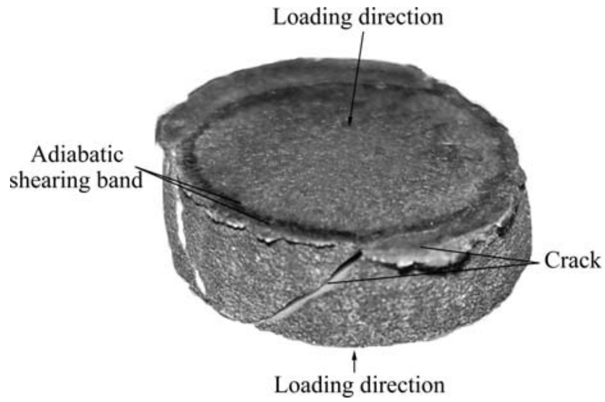

Fig.4 Schematic representation of fracture features and orientation of ASB

Due to the short duration of high intensity stresses generated by transient stress waves, the heat generated by plastic work in the localized regions can be hardly transferred and the process becomes nearly adiabatic. The temperature rise gives local softening, while the surrounding material continues to be hardened. When being further loaded, if the thermal softening overcomes the strain and strain rate hardening, the deformation takes place in bands of intense plastic shear, which form ASB. Fig.5(a) shows the optical micrograph of the arc-type ASB for a specimen deformed at 300 ℃ and 5 800 s^{-1}. An adiabatic temperature rise within the localized shear band impels the rotation dynamic recrystallization (RDR)[17] which occurs in the ASB in Fig.5(b), where a number of fine equiaxed recrystallized grains are distributed.

For the ductile metals, the damage and fracture process involves a number of metallurgical events such as nucleation, growth and coalescence of microvoids. During high strain rate impact, due to the large strain in ASBs, the microvoids develop easily in these regions and grow under high mean stresses rapidly. Microvoid's coalescence is controlled by the localized plastic flow

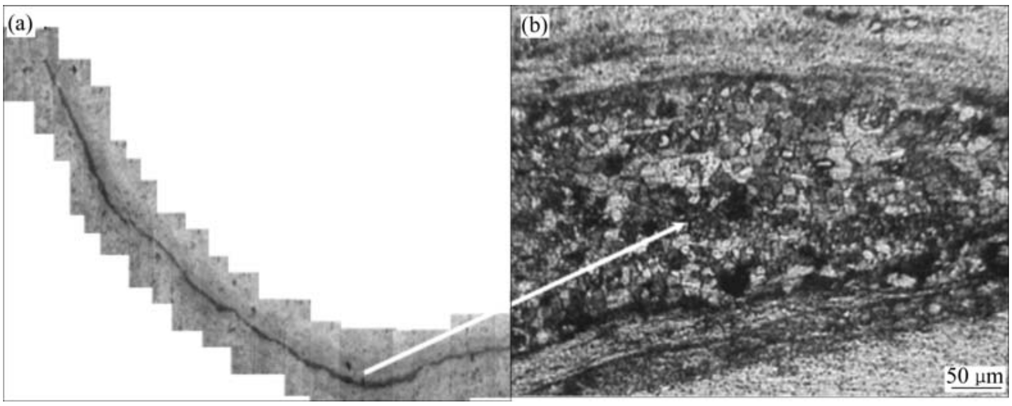

Fig.5 Adiabatic shear band in specimen impacted at 300 ℃ and 5 800 s^{-1}: (a) Optical micrograph showing arc-type ASB; (b) Fine equiaxed recrystallized grains

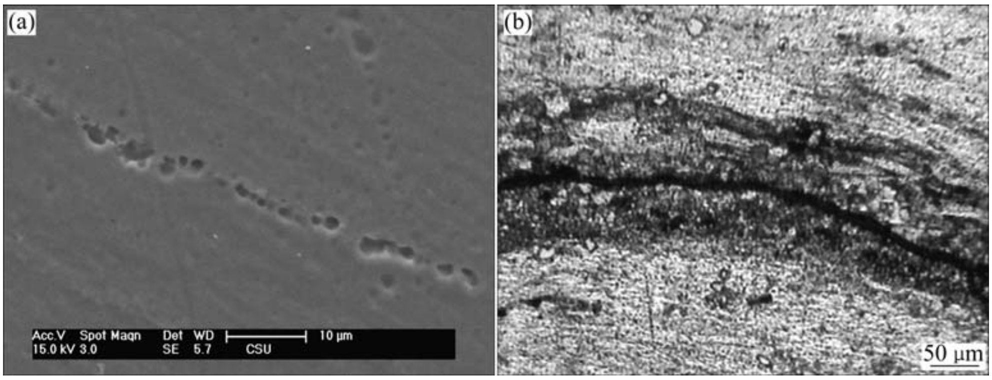

Fig.6 Specimen impacted at 300 ℃ and 5 800 s^{-1}: (a) Coalescence of voids observed by SEM; (b) Cracking along ASB by OM

around them, which is shown in Fig.6(a). Such coalescence of microvoids results in a progressive reduction of the strength when the damage reaches a critical stage where the void coalescence forms a cracking and fracture can happen. From Fig.6(b), it can be seen that cracks are extended along the ASBs.

4 Conclusions

1) Aluminum alloy 2519A-T87 plate is impacted at temperatures of 150, 300 and 450 ℃. When the impacts occur at the strain rate of 630 s^{-1}, an increasing strain causes an increase of the flow stress. At strain rate of 4 300 s^{-1}, the stress reaches its peak followed by a steady state deformation. At strain rate of 5 800 s^{-1}, the stress reaches its peak followed by a decrease with an increasing strain due to the adiabatic shearing thermal-plastic instability.

2) The strain rate sensitivity exponents m determined are 0.066, 0.059 4, 0.059 0 and 0.057 3 at temperatures of 20, 150, 300 and 450 ℃, respectively. By means of the experimentally determined material parameters, the Cowper-Symonds overstress power law constitutive equation of aluminum alloy 2519A satisfies

$$Y_{\mathrm{d}} = 420\left[1+\left(\frac{\dot{\varepsilon}}{147\,394.015\,41}\right)^{1/3.203\,71}\right]$$

3) Fractographic analysis shows that ASB plays a key role in the dynamic failure process of 2519A alloy. Inhibiting the formation and propagation of ASB is an effective approach to improve the dynamic performances of 2519A.

References

[1] LI H Z, ZHANG X M, CHEN M A. Hot deformation behavior of 2519 aluminum alloy [J]. The Chinese Journal of Nonferrous Metals, 2005, 15(4): 621−625. (in Chinese)

[2] LIN Q Q, ZHANG H, PENG D S. Feature of flow stress of 2519 aluminum alloy during hot compressive deformation [J]. Mining and Metallurgical Engineering, 2002, 22(2): 110−113. (in Chinese)

[3] SIA N N, JON B I, JOHN E S. Hopkinson techniques for dynamic recovery experiments [J]. Proc R Lond A, 1991, 25: 371−391.

[4] LEE O S, KIM M S. Dynamic material property characterization by using split Hopkinson pressure bar (SHPB) technique [J]. Nuclear Engineering and Design, 2003, 226: 119−125.

[5] SMERD R, WINKLER S, SALISBURY C, WORSWICK M, LLOYD D, FINN M. High strain rate tensile testing of automotive aluminum alloy sheet [J]. International Journal of Impact Engineering, 2005, 32: 541−560.

[6] ARILD H C, TORE B, ODD S H, AHMED B. Flow and fracture characteristics of aluminum alloy AA5083-H116 as function of strain rate, temperature and triaxiality [J]. Mater Sci Eng A, 2004, 364: 260−272.

[7] TORE B, ARILD H C, MAGNUS E, TORODD B, ODD S H. Experimental and numerical study on the perforation of AA6005-T6 panels [J]. International Journal of Impact Engineering, 2005, 32: 35−64.

[8] LEE W S, SUE W C, LIN C F, WU C J. Strain rate and temperature dependence of the dynamic impact properties of 7075 aluminum alloy [J]. Journal of Materials Processing Technology, 2000, 100: 116−122.

[9] STELLY M J, LE G. Shock waves and high strain-rate phenomena in metals [M]. New York: Plenum Press, 1981: 113.

[10] LEE W S, LIN C F, LIU C Y, TZENG F T. Impact properties of 304L stainless steel GTAW joints evaluated by high strain rate of compression tests [J]. Journal of Nuclear Materials, 2004, 335: 335−344.

[11] TORE B, HOPPERSTAD O S, BERSTAD T, LANGSETH M. A computational model of viscoplasticity and ductile damage for impact and penetration [J]. Eur J Mech A/Solids, 2001, 20: 685−712.

[12] WANG L L. Foundations of stress waves [M]. Beijing: National Defense Industry Press, 2005: 52−60. (in Chinese)

[13] LINDHOLM U S, BESSEY R L. Effect of strain rate on yield strength, tensile strength, and elongation of three aluminum alloys [J]. Journal of Materials Science, 1971, 6(1): 119−233.

[14] OOSTERKAMP L. High strain rate properties of selected aluminum alloys [J]. Mater Sci Eng A, 2000, 278: 225−235.

[15] HALLQUIST J O. LS-DYNA keyword user's manual v970 [M]. California: Livermore Software Technology Corporation, 2003: 150−200.

[16] YU T X, LU G X. Energy absorption of structures and materials [M]. Beijing: Chemical Industry Press, 2006: 42. (in Chinese)

[17] ANDRADE U, MEYERS M A. Dynamic Recrystallization in high-strain-rate plastic deformation of copper [J]. Acta Metall Mater, 1994, 42(9): 3180−3183.

(Edited by LI Xiang-qun)